

## Multidisciplinary Design Optimization of Long Endurance Unmanned Aerial Vehicle Wing

S. Rajagopal<sup>1</sup> and Ranjan Ganguli<sup>2</sup>

**Abstract:** The preliminary wing design of a low speed, long endurance UAV is formulated as a two step optimization problem. The first step performs a single objective aerodynamic optimization and the second step involves a coupled dual objective aerodynamic and structural optimization. During the first step, airfoil geometry is optimized to get maximum endurance parameter at a 2D level with maximum thickness to chord ratio and maximum camber as design variables. Leading edge curvature, trailing edge radius, zero lift drag coefficient and zero lift moment coefficient are taken as constraints. Once the airfoil geometry is finalized, the wing planform parameters are optimized with minimization of wing weight and maximization of endurance. Four design variables from aerodynamics discipline namely taper ratio, aspect ratio, wing loading and wing twist are considered. Also, four more design variables from the structures discipline namely the upper and lower skin thicknesses at root and tip of the wing are added. Constraints are stall speed, maximum speed, rate of climb, strength and stiffness. The 2D airfoil and 3D wing aerodynamic analysis is performed by the XFLR5 panel method code and the structural analysis is performed by the MSC-NASTRAN finite element code. In the optimization process, a multi-objective evolutionary algorithm named NSGA-II (non-dominated sorting genetic algorithm) is used to discover the full Pareto front for the dual objective problem. In the second step, in order to reduce the time of computation, the analysis tools are replaced by a Kriging meta-model. For this dual objective design optimization problem, numerical results show that several useful Pareto optimal designs exist for the preliminary design of UAV wing.

**Keywords:** Unmanned Aerial Vehicle, Multidisciplinary design optimization, multi-objective optimization, genetic algorithm, Pareto front, Kriging

---

<sup>1</sup> Corresponding author; E-mail: raja@aero.iisc.ernet.in; Address: CTC Division, ADE, DRDO, Govt of India, New Thippasandra Post, Bangalore-560075, India; Phone: +918025057242; Fax: +918025283188.

<sup>2</sup> Email: ganguli@aero.iisc.ernet.in; Phone: +918022933017; Fax: +918023600134

## Abbreviations

<i>UAV</i>	Unmanned Aerial Vehicle
$\bar{x}$	Design variable
$\bar{g}$	Inequality constraint
$C_l$	2D Lift coefficient for airfoil
$C_d$	2D drag coefficient for airfoil
$C_{m0}$	2D zero lift moment coefficient for airfoil
$C_{m0}^*$	Maximum allowable 2D zero lift moment coefficient for airfoil
<i>TC</i>	Thickness to Chord ratio of wing in percentage
<i>MC</i>	Mean camber line of the airfoil cross-section
<i>LEC</i>	Leading Edge Curvature of airfoil cross-section
<i>LEC*</i>	Maximum allowable Leading Edge Curvature of airfoil cross-section
<i>TER</i>	Trailing edge angle of the airfoil cross-section
<i>t</i>	Endurance in hrs
<i>WW</i>	Wing Weight in kg
<i>AR</i>	Wing Aspect Ratio
<i>TR</i>	Wing Taper Ratio
<i>WL</i>	Wing Loading in kg/m <sup>2</sup>
<i>HCR</i>	Loiter Altitude in m
<i>ROC</i>	Rate of Climb in m/s
$C_L$	3D Lift coefficient for wing
$C_D$	3D drag coefficient for wing
<i>VMAX</i>	Maximum Speed in kmph
<i>VMAX*</i>	Maximum allowable Maximum Speed at sea-level in kmph
<i>VS</i>	Stall Speed in kmph
<i>VS*</i>	Maximum allowable Stall Speed at sea-level in kmph
$\sigma$	Von-mises stress in kg/m <sup>2</sup>
$\sigma^*$	Maximum allowable Von-mises stress in kg/m <sup>2</sup>
$\delta$	Maximum displacement on the wing in m
$\delta^*$	Maximum allowable Maximum displacement on the wing in m

## 1 Introduction

Aircraft design is an ideal candidate for Multidisciplinary Design Optimization (MDO), since it governed by four major disciplines: aerodynamics, structure, control and propulsion. A conventional aircraft design process starts with aerodynamic design to satisfy the performance requirements and is followed by design iterations and checks to satisfy requirements from other disciplines such as structures. In contrast, a good optimal design handles all the inputs from various disciplines and

performs an interdisciplinary trade off. Nowadays, aircraft designers are looking for such an optimal solutions through MDO.

In the aircraft design field, many optimization works have been carried out over the last 30 years. These works primarily focus on obtaining the best aerodynamic or structural design. Over the last decade, designers have applied MDO to aircraft design as described by Sobieski and Haftka (1996), Bartholomew (1998) and Kroo (1997). The survey of developments by Sobieski and Haftka (1996) reports that MDO methodology has transcended its structural optimization roots and is growing in scope and depth toward encompassing the complete set of disciplines required by applications. According to that survey, the two major obstacles in realizing the full potential of MDO technology appear to be the high computational demands and complexities arising from organization of the MDO task.

Bartholomew (1998) provides a definition of MDO and discusses the function of MDO as a key tool in the context of concurrent engineering. He also says that MDO permits the constraints of a diverse range of disciplines to be addressed from an early stage of the design process. Kroo (1997) highlights some important aspects of MDO applications in the preliminary design phase. Kroo also covers the evolution of computational tools, strategies and challenges. Most of the researchers focus mainly on applying MDO to the complete aircraft design during its conceptual design stage [Sobester and Keane (2006); Rajagopal, Ganguli, Pillai and Lurdharaj (2007)] and to the design of wing [Grossman, Haftka, Kao, Polen and Rais-Rohani (1990)] during the preliminary design phase. Sobester and Keane (2006) constructed a multidisciplinary analysis for UAV airframes. They consider a blended wing body design and illustrate optimization of the geometry using a constraint analysis. Rajagopal Ganguli, Pillai and Lurdharaj (2007) formulated the conceptual design of an UAV as an optimization problem and performed the initial aircraft sizing through the optimization approach. During the conceptual design phase, the analysis is often done using low fidelity analysis tools such as empirical relations. Hence the MDO approach does not demand large computing power and time. On the other hand, during the preliminary design phase, high fidelity analysis tools such as Computational Fluid Dynamics (CFD), Finite Element Method (FEM) etc. are used which demand enormous computing power and time. Moreover, the coupling between the disciplines increases during preliminary design phase thereby increasing the time and power of computation.

Much research in the field of aircraft design using the MDO approach has focused on applying MDO for conventional commercial transport aircraft and current generation fighters. Grossman, Haftka, Kao, Polen and Rais-Rohani (1990) integrated aerodynamic and structural design of a subsonic transport wing for minimum weight subject to a constraint on range. They recommended two methods

to alleviate the computational burden. The first method called the modular sensitivity methods reduces the cost of calculating the sensitivity derivatives and allows the usage of black box disciplinary software packages. They showed in the study that derivatives of the aeroelastic response and divergence speed can be calculated without the costly computation of derivatives of aerodynamic influence coefficient and structural stiffness matrices. The second approach to reduce the computational cost involved use of sequential approximate optimization. Dovi and Wrenn (1990) provided an envelope function formulation that converts a constrained optimization problem into an unconstrained one. The advantage of this new method for multi-objective optimization is the elimination of separate optimization for each objective, which is required by some optimization methods. A typical wide body transport aircraft was used for comparison studies. The method was compared with the Penalty function method and Global Criterion method and was found to be superior. Wakayama and Kroo (1995) performed wing planform optimization for minimum drag with constraints on structural weight and maximum lift. The study gave the basic influence of drag, weight and maximum lift on optimal wing planform. It was observed that induced drag and structural considerations strongly favor highly tapered wings to attain large spans. Moreover, parasite and compressibility drag have limited effect on wing taper, making maximum lift constraints necessary for generating realistic tip chords.

Martins and Alonso (2002) demonstrated a new integrated aerodynamic structural design method for aerospace vehicles. They employed high fidelity models for both aerodynamic and structural disciplines and also used a high fidelity coupling procedure. Euler equations were used for aerodynamic analysis and a detailed FEM model for the primary structure. Carrier (2004) describes the MDO system implemented at ONERA. It contains different optimization algorithms including a gradient based optimizer and a GA. The two disciplines of aerodynamics and structures are analyzed with high fidelity methods whereas the other disciplines such as engine performance and flight mechanics are evaluated with simpler methods. This system was applied for optimizing the performance of a high-speed civil transport aircraft. The overall objective was to maximize the aircraft range while multiple design constraints are considered. Kumano, Jeong and Obayashi (2006) describe the MDO system for a small jet aircraft design by integrating the CFD codes and NASTRAN based aeroelastic structural interface code. They employ a kriging model to save computational time of objective function evaluation in the multi-objective genetic algorithm (MOGA). Several non-dominated solutions indicating the trade off among the drag, structural weight, drag divergence and pitching moment were found. Kim, Jeon and Lee (2006) found an aerodynamic/structural multidisciplinary design with multiple objectives for a supersonic fighter wing us-

ing response surface methodology. Nine wing and airfoil parameters were chosen for the aerodynamic design variables and four structural variables were added to determine the wing skin thickness. To consider various flight conditions, multi-point design optimization was performed on the three representative design points. Morino, Bernardini and Mastroddi (2006) used MDO for the conceptual design of innovative aircraft configurations based on the integrated modeling of structures, aerodynamics, and aeroelasticity.

Researchers have applied optimization methodology to specific disciplines like aerodynamics to address specific, complex and critical issues such as low Reynolds number flows. Srinath and Mittal (2009) studied the flow over NACA 0012 airfoil at two different angle of attacks for Reynolds numbers less than 500. It was seen that the flow is very sensitive to Reynolds number. A continuous adjoint based method was formulated and implemented for the design of airfoils at low Reynolds numbers. Kipouros, Jaeggi, Dawes, Parks, Savill, and Clarkson (2008) demonstrated the application of a novel multi-objective variant of the Tabu Search optimization algorithm to the aerodynamic design optimization of turbomachinery blades.

In recent years, UAV's have gained the attention of aerospace engineers for use in reconnaissance roles related to counter terrorism. Some unique opportunities are provided by UAV design as compared to the conventional manned aircraft design, especially more flexibility in the selection of wing design parameters. Some recent research activity has focused on UAV applications. Gonzalez, Lee, Srinivas and Wong (2006) discuss the use of evolutionary algorithms (EA) for a single and multi-objective airfoil optimization. They bring out the demerits of applying the gradient based approach for problems involving multi-objective, multi-modal and non-differentiable functions. They show that EA's have the capability to find global optimum and can be executed in parallel. In another work, Gonzalez, Periaux, Srinivas and Whitney (2006) highlight the difficulties in the design of UAV's arising due to the varied and non-intuitive nature of the configurations and missions that can be performed by these vehicles. An MDO framework was applied and two case studies were performed using high fidelity analysis codes. The first case study involves dual objective UAV airfoil section optimization. Detailed design of a single element airfoil for a small UAV application similar to the RQ-7A Shadow 200 tactical UAV was performed with the two fitness functions defined as minimization of drag at two different flight conditions. Three constraints for maximum thickness, maximum thickness location and pitching moment were used. In the second case study, multi-criteria wing design optimization for a UAV with the two fitness functions defined as minimization of wave drag and minimization of the spanwise cap weight was performed. Constraints were imposed on minimum thickness and position of maximum thickness. Similarly, Lee, Gonzalez, and Srinivas (2008) have

developed robust evolutionary algorithms for UAV/UCAV aerodynamic and RCS design optimization. Here, the prime objective was to improve the survivability and aerodynamic efficiency. The research of Srinivas and co-workers represents a pioneering effort in the use of MDO for UAV design.

We see that some research has been done on the design optimization of UAV's. However, the use of MDO in UAV designs is much less compared to its use in conventional manned aircraft. This is especially true for the application of evolutionary algorithm to UAV design. Also, most works use simple GA for the optimization problem and have not exploited the power of evolving multi-objective GAs. The advantages of evolutionary methods over classical algorithms in single and multi-objective optimization problems are well highlighted by Goldberg (1989) and Deb (2001), respectively. This paper investigates the preliminary design of an UAV wing as an optimization problem. Evolutionary algorithms, which capture the full Pareto Front for multi-objective problems are used in conjunction with a Kriging meta-model of the analysis. A low speed, long endurance UAV is illustrated.

## 2 Problem Formulation

The preliminary design of the UAV under consideration focuses on achieving its main goal i.e. the long endurance and minimum structural weight. The fuselage design is usually governed by the amount of the fuel to be carried and the volume of systems like payload and equipment. Therefore, only the wing design is considered for the optimization problem. In the optimization process, the design aims at maximizing the endurance, which is an aerodynamic aspect and minimizing the wing weight, which is a structural aspect. The optimization problem involves objective functions, design variables and constraints. The same optimizer is used for both single and dual objective problems.

### 2.1 Objective functions

The choice of the objective function in any aircraft optimization problem is dictated by the design mission of the aircraft. Since the design mission of the UAV under consideration is long endurance, the main objective is chosen as endurance while formulating the optimization problem. Also, achieving minimum structural weight is a general challenge for aircraft designers. Therefore, minimization of wing weight is also considered as another objective for the optimization problem. Since the aerodynamic analysis of the wing is performed in two steps, the optimization methodology is also performed in two parts namely the 2D airfoil optimization and 3D wing optimization. In the 2D airfoil optimization, the airfoil geometry is optimized with a single objective of maximizing the endurance parameter

( $C_l^{3/2}/C_d$ ). The lift and drag characteristics correspond to the 2D characteristics of the airfoil. In the 3D wing optimization, the wing planform parameters are optimized with dual objectives. The first objective function is the maximization of the endurance parameter ( $C_L^{3/2}/C_D$ ), which reflects the aerodynamic discipline. Here the lift and drag characteristics correspond to that of the wing. The second objective function is minimization of the wing weight and reflects the structures discipline.

## 2.2 Design Variables

The design space is chosen to reflect the effect of aerodynamic and structural disciplines. In this study, the wing parameters related to planform, the airfoil shapes and the structural skin thicknesses are identified as the design variables, as summarized in Table 1. Usually, apart from the skin thicknesses the spar cap thickness, is also included for optimization problem. But in order to keep the optimization simpler with less number of design variables, the spar cap thickness is not included in the current optimization problem. The design variables for the 2D airfoil optimization are the first two parameters described in Table 1: the maximum wing thickness to chord ratio and the maximum camber.

The remaining eight parameters are additional design variables included for the 3D wing optimization. The 2D design optimization uses 2 design variables while the 3D design optimization uses 8 additional design variables. The design variables are also explained in detail in Fig 1. Throughout this paper, the design variables are normalized and presented as ratios with respect to the upper bound value.

## 2.3 Constraints

Aerodynamic constraints are imposed on the performance parameters of the UAV and on the airfoil shape. For the 2D airfoil optimization, the aerodynamic constraints are imposed on the leading edge curvature (LEC), trailing edge angle (TER), zero drag and zero moment co-efficient. Moreover, for the 3D wing optimization, the aerodynamic constraints are imposed on (1) rate of climb (ROC) at that altitude, (2) stall speed (VS) and (3) maximum speed (VMAX) at sea level condition, which arise from the requirements. The structural constraints imposed are based on the strength and stiffness of the wing. The maximum stress coming on the wing structure should be less than the allowable bending stress of the material. This condition is imposed as the strength constraint. As per the AVP 970 standard, the maximum wing deflection allowed for an UAV for 1g condition is 1% of the span. This condition is imposed as the stiffness constraint.

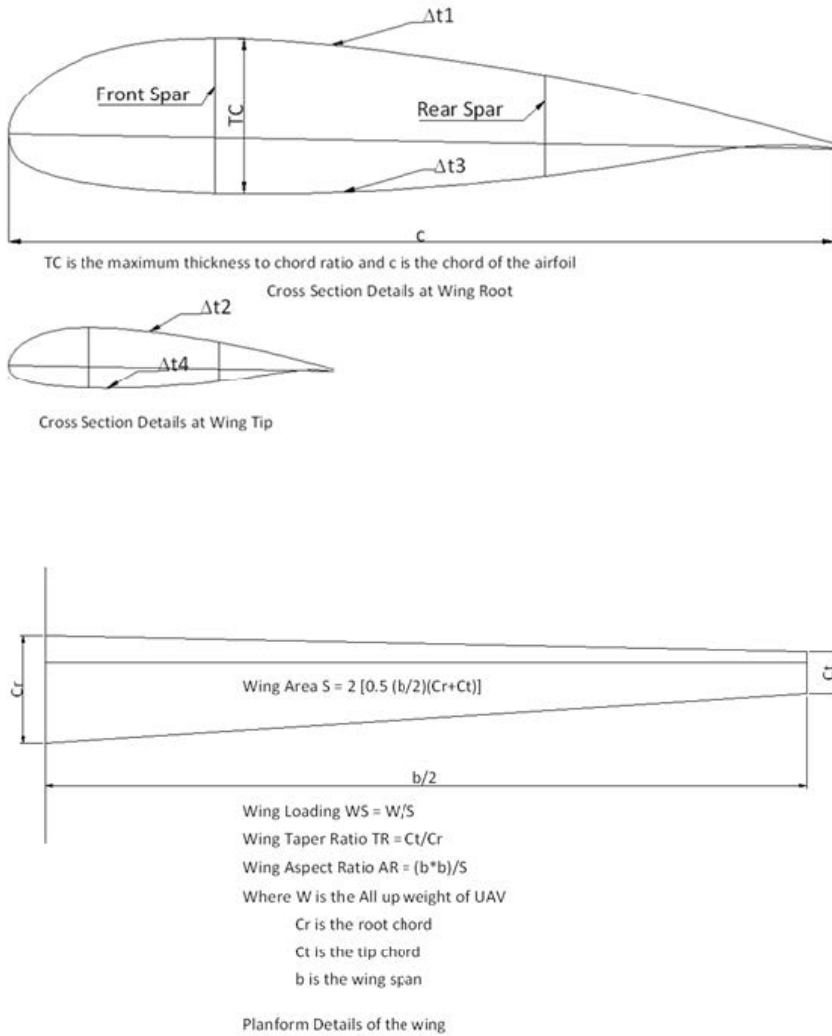


Figure 1: Schematic representation of the design variables

**2.4 Mathematical Representation of 2D airfoil Design Problem**

The 2D airfoil design problem can be written as a standard optimization problem:

$$Maximize f(\bar{x}) = Maximize \left[ \frac{C_l^{3/2}}{C_d} \right] \tag{1}$$



Table 1: Design Variables. Normalized with Upper Bounds

No	Design Variables	Notation	Usage	Lower Bound	Baseline Design
1	Maximum Wing Thickness to chord Ratio	TC	2D	0.727	0.77
2	Maximum camber	MC	2D	0	0.2
3	Wing Aspect Ratio	AR	3D	0.727	0.73
4	Wing Loading	WS	3D	0.6	0.7
5	Wing Taper Ratio	TR	3D	0.25	0.5
6	Wing twist angle	$\theta$	3D	0	0.6
7	Upper skin thickness at root	$\Delta t_1$	3D	0	0.8
8	Upper skin thickness at tip	$\Delta t_2$	3D	0	0.8
9	Lower skin thickness at root	$\Delta t_3$	3D	0	0.8
10	Lower skin thickness at tip	$\Delta t_4$	3D	0	0.8

Subject to

$$\bar{g}_1(\bar{x}) = [LEC(\bar{x}) - LEC^*] \leq 0 \quad (2)$$

$$\bar{g}_2(\bar{x}) = [-TER(\bar{x}) + TER^*] \leq 0 \quad (3)$$

$$\bar{g}_3(\bar{x}) = [C_{m_0}(\bar{x}) - C_{m_0}^*] \leq 0 \quad (4)$$

$$x_l \leq \bar{x} \leq \bar{x}_u \quad (5)$$

$$\bar{x} = [TC \quad MC]^T \quad (6)$$

The 2D optimization problem has one objective function, three constraints and two design variables. Only the aerodynamics discipline is involved in this problem.

## 2.5 Mathematical Representation of 3D wing Design Problem

The 3D wing design problem can be written as a standard optimization problem:

$$\text{Maximize } f(\bar{x}) = \text{Maximize} \begin{bmatrix} \frac{C_L^{3/2}}{C_D} \\ -WW(\bar{x}) \end{bmatrix} \quad (7)$$

Subject to

$$\bar{g}_1(\bar{x}) = [-ROC(\bar{x}) + ROC^*] \leq 0 \quad (8)$$

$$\bar{g}_2(\bar{x}) = [VS(\bar{x}) - VS^*] \leq 0 \quad (9)$$

$$\bar{g}_3(\bar{x}) = [-VMAX(\bar{x}) + VMAX^*] \leq 0 \quad (10)$$

$$\bar{g}_4(\bar{x}) = [\sigma(\bar{x}) - \sigma^*] \leq 0 \quad (11)$$

$$\bar{g}_5(\bar{x}) = [\delta(\bar{x}) - \delta^*] \leq 0 \quad (12)$$

$$\bar{x}_l \leq \bar{x} \leq \bar{x}_u \quad (13)$$

$$\bar{x} = [AR \quad WS \quad TR \quad \theta \quad \Delta t1 \quad \Delta t2 \quad \Delta t3 \quad \Delta t4]^T \quad (14)$$

The 3D optimization problem has two objective functions, seven constraints and eight design variables. It involves multi-objective optimization. Both aerodynamic and structural disciplines are involved in this problem.

### 3 Analysis

As the optimization problem involves analysis in the aerodynamics and structures discipline, the mathematical model consists of two key components namely (i) Aerodynamic analysis and (ii) Structural analysis. These analysis procedures are briefly described below.

#### 3.1 Aerodynamic Analysis

The panel method code XFLR5 is considered for the aerodynamic analysis. Basically, XFLR5 is a user friendly interface for the XFOIL code developed by Drela (2001). The XFOIL code uses a higher order panel method with coupled integral boundary layer. The algorithms for foil analysis implemented in XFLR5 are exactly the same as those of the original XFOIL code, except for the translation from FORTRAN to C++.

The inviscid formulation of XFOIL is a simple linear-vorticity stream function panel method. A finite trailing edge base thickness is modeled with a source panel. The equations are closed with an explicit Kutta condition. A Karman-Tsien compressibility correction is incorporated, allowing good compressible predictions all the way to sonic conditions. The theoretical foundation of the Karman-Tsien correction breaks down in supersonic flow, and as a result accuracy rapidly degrades as the transonic regime is entered. Of course, shocked flows cannot be predicted with any certainty. However, the UAV considered in this paper operates in flight conditions which satisfy the assumptions of the code.

As far as the viscous formulation is concerned, the boundary layers and wake are described with a two-equation lagged dissipation integral BL formulation and an

envelope end transition criterion, both taken from the transonic analysis/design ISES code. The entire viscous solution (boundary layers and wake) is strongly interacted with the incompressible potential flow via the surface transpiration model (the alternative displacement body model is used in ISES). This permits proper calculation of limited separation regions. The drag is determined from the wake momentum thickness far downstream. A special treatment is used for a blunt trailing edge which fairly accurately accounts for base drag. The total velocity at each point on the airfoil surface and wake, with contributions from the freestream, the airfoil surface vorticity, and the equivalent viscous source distribution, is obtained from the panel solution with the Karman-Tsien correction added. This is incorporated into the viscous equations, yielding a nonlinear elliptic system which is readily solved by a full-Newton method as in the ISES code.

If lift is specified, then the wake trajectory for a viscous calculation is taken from an inviscid solution at the specified lift. If angle of attack is specified, then the wake trajectory is taken from an inviscid solution at that angle of attack. This is not strictly correct, since viscous effects will in general decrease lift and change the trajectory. This secondary correction is not performed, since a new source influence matrix would have to be calculated each time the wake trajectory is changed. This would result in unreasonably long calculation times. The effect of this approximation on the overall accuracy is small, and will be felt mainly near or past stall, where accuracy tends to degrade anyway. In attached cases, the effect of the incorrect wake trajectory is imperceptible.

Also, wing analysis capabilities using the Vortex Lattice Method (VLM) are added in the XFLR5 code. The wing is defined as a set of panels. Each panel is defined by its length, its root and tip chords, by its dihedral angle and by its mesh for VLM analysis. Twist is processed as a modification of the angle of attack as given in the guidelines for XFLR5 V2 Rev 5. As discussed in the guidelines, the principle of a VLM is to assimilate the perturbation generated by the wing to that of a sum of vortices distributed over the wing's planform. The strength of each vortex is calculated to meet the appropriate boundary conditions, i.e. non-penetration conditions on the surface of the panels. The induced drag is calculated by integration of surface forces at the  $3/3$  point of the VLM panels. The viscous drag is estimated by interpolation of XFOIL pre-generated polars from the  $C_l$  value resulting from the linear VLM analysis.

The aerodynamic analysis is performed in two parts: the 2D airfoil analysis and the 3D wing planform analysis. Both these analysis are performed using the XFLR5 code where the 2D airfoil analysis is exactly same as that of the XFOIL code and the 3D wing analysis is done using the VLM method. These codes are well validated with wind tunnel test experiments and other CFD codes.

The performance constraints are evaluated using the commercially available and well-validated aircraft design software RDS based on the book by Raymer (2001) on the aircraft design, which is introduced after the XFLR5 code. The sizing and synthesis analysis of this software is well-validated for many aircraft conceptual design stage applications. The RDS has a propulsion module that generates the thrust data. The aerodynamic characteristics evaluated by the XFLR5 are used by the performance module of RDS that evaluates the performance constraints. As far as the XFLR5 code is concerned, the points where it does not converge are ignored, during the optimization routine.

### **3.2 Structural Analysis**

In this research, the commercially available and well validated FEM code MSC-NASTRAN developed by MSC Software Inc. is used for the structural analysis of the wing. This software is used to perform the analysis and estimate the wing weight. For carrying out the structural analysis using the FEM code MSC-NASTRAN, the geometry is modeled using commercially available and well validated CAD software CATIA developed by Dassault Systems. This software is used to generate the model geometry in the CAD environment and this geometric model is read by the commercially available and well validated mesh generation code MSC-PATRAN developed by MSC Software Inc. The mesh generated by this software is analyzed using the FEM solver MSC-NASTRAN.

The structural model is developed by dividing the entire structure into a number of discrete elements. The basic steps required to perform the structural analysis using FEM solver MSC-NASTRAN are as follows:

- The continuous structure is represented as a collection of nodal points connected by discrete elements
- From the given element properties, material properties and geometry, the elemental stiffness matrices are formulated
- The global stiffness matrix corresponding to the full structure is assembled from the elemental stiffness matrices
- The boundary conditions are applied to constrain the model and the load vectors are generated
- The static equilibrium matrix  $\{f\}=[K]\{d\}$  where  $K$  is the system stiffness,  $f$  is the load vector and  $d$  is the nodal displacement vector is solved. The unknowns are the nodal displacements which are evaluated by inverting the stiffness matrix and multiplying by the force vector.

- Other required outputs like strains and stresses can be derived from the nodal displacements.

The geometry, loads and boundary conditions, material properties are captured in the pre-processor MSC-PATRAN. The meshing is also carried out in the pre-processor itself. For the baseline model in the structural analysis, the wing is made of three parts in the chordwise direction namely the leading edge box, center section and the trailing edge box. For the optimization problem, only the center box is considered. The center box consists of upper and lower skin and front and rear spars. The upper and lower skin thicknesses at root and tip are considered as the design variables. The structural model is created in MSC-PATRAN with loads and boundary conditions. The element chosen for modeling the wing structure is the general shell element. Only one half of the wing is modeled with symmetric boundary conditions at the root of the wing. All the six degrees of freedom of the nodes at the root of the wing takes the values as  $U_Z=0$ ,  $ROT_X=0$ ,  $ROT_Y=0$ . Also, in order to arrest the rigid body motion of the wing, only node at the wing root takes the boundary condition  $U_X=0$ ,  $U_Y=0$ . The air loads as generated by the aerodynamic analysis code XFLR5 are given in each element of the wing as pressure load. The self weight of the wing structure is also taken into consideration which gives a weight (inertia) relief for the structure. The wing is a sandwich construction made up of CFRP skin with Rohacell foam core with epoxy resin system. The material properties are defined in MSC-PATRAN. The material properties considered for this optimization problem are tabulated in Table 2. The modeling of the composite materials is carried out in LAMINATE MODELLER module of the MSC-PATRAN and is modeled layerwise. The properties given in Table 2 are experimental tested values of one layer of fabric along with the resin system. Fig 2 gives the FEM model created in the MSC-PATRAN.

#### 4 Optimization

The optimization process is performed in two steps. First, the airfoil is finalized through a single objective optimization problem. Once the airfoil is frozen, the wing planform parameters are arrived at through a dual objective problem. The optimization model is illustrated in Fig. 3 and is composed of different modules namely the mesh module, analysis module, meta-model module and optimization module. For the first step, the analysis module includes only the aerodynamic analysis which is performed by the XFLR5 code. For the second step, the analysis module includes both the aerodynamics and structural analysis.

Large computer time remains the biggest challenge in solving any MDO problem. The computation time increases because of the strong interactions between the dis-

Table 2: Properties of structural material considered for the wing

S No	Property	Unit	CFRP- Unidirectional Fabric	CFRP – Bidirectional Fabric	Rohacell R51
1	Tensile strength in Longitudinal direction	Kg/mm <sup>2</sup>	92	35	0.19
2	Tensile strength in Transverse direction	Kg/mm <sup>2</sup>	15	35	-
3	Compressive Strength in Longitudinal direction	Kg/mm <sup>2</sup>	92	30	0.09
4	Compressive Strength in Transverse direction	Kg/mm <sup>2</sup>	15	30	-
5	Shear Strength	Kg/mm <sup>2</sup>	5	4	0.08
6	ILSS	Kg/mm <sup>2</sup>	4	4	-
7	Young's Modulus in Longitudinal Direction	Kg/mm <sup>2</sup>	12000	6500	7
8	Young's Modulus in Transverse Direction	Kg/mm <sup>2</sup>	300	6500	7
9	Shear Modulus	Kg/mm <sup>2</sup>	400	350	2.1
10	Poisson's Ratio	-	0.2	0.2	0.2
11	Density	g/cc	1.6	1.4	0.05

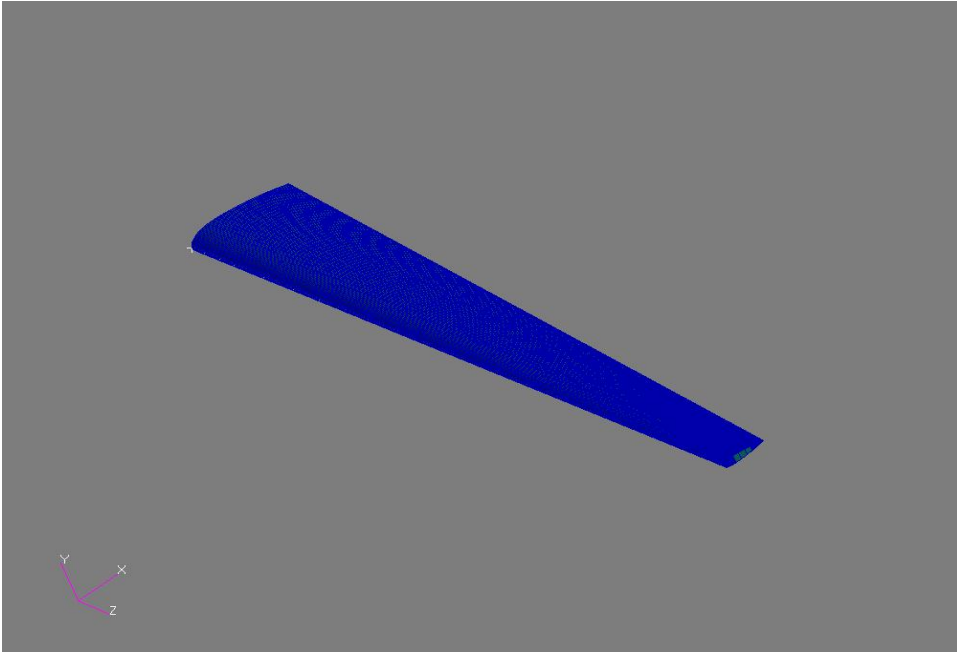


Figure 2: FEM Model of the 3D wing created in MSC-PATRAN

ciplines and the use of high fidelity codes for aerodynamic and structural analysis. Such codes typically solve partial differential equations through discretization methods in a procedure which is computationally intensive. Fortunately, the computation time can be drastically reduced if accurate approximate models to replace the analysis tools can be created. Such models of models, or meta-models, are very useful in optimization. For example, the response surface method described by Kim, Jeon and Lee (2006) and Kriging model explained by Kumano, Jeong and Obayashi (2006) have been successfully applied for MDO problems. While response surface methods use polynomial expressions which are locally valid, Kriging is suited to approximate highly nonlinear functions and can be used to create globally valid meta-models. In the present study, Kriging model is employed for design of the UAV wing. The meta-model module generates the Kriging model and validates for sample points.

#### **4.1 Kriging Model**

Kriging model has its original roots in the field of geostatistics which is a mixed discipline of mining, engineering, geology, mathematics and statistics. In this field, this meta-model is used to predict temporal and spatial correlated data. A wide

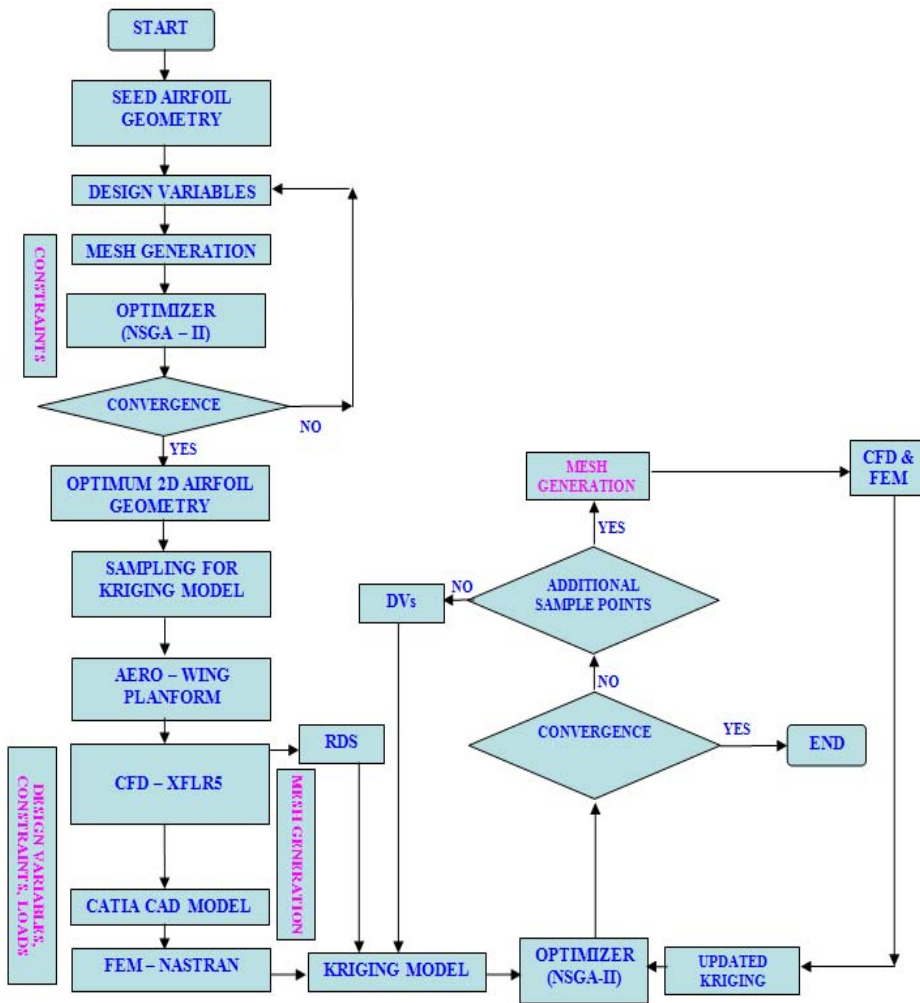


Figure 3: UAV Design Optimization Process

range of correlation functions can be chosen for building the meta-model thereby making the Kriging meta-models extremely flexible.

The analysis tool is replaced with the Kriging model in the objective function evaluation process of MOGA. As the Kriging model introduces uncertainty at the prediction point, the biggest advantage of GA in obtaining the global optimization may be lost as studied by Jeong, Murayama and Yamamoto (2005). In order to



retain this advantage, both the prediction value and its uncertainty are to be considered at the same time. This is captured by updating the Kriging model during the optimization. If the optimization algorithm is not converged, additional random designs are initialized and the Kriging model is reconstructed. The Gaussian correlation function used in the meta-model interpolates all data points exactly. Kriging model takes a combination of a polynomial model and a statistical function and is written as follows,

$$y(x) = f(x) + z(x)$$

where  $y(x)$  is the unknown function,  $f(x)$  is the known polynomial function and  $z(x)$  is the function from a stochastic process with mean zero, variance and non-zero covariance. The polynomial function  $f(x)$  approximates the design space globally and the localized deviations are created by the function  $z(x)$ . The polynomial function is taken as a constant term for this study. The covariance matrix of  $z(x)$  that is responsible for the local deviations is,

$$\text{Cov}[z(x^i), z(x^j)] = \sigma^2 R([R(x^i, x^j)])$$

where  $R$  is the correlation matrix, and  $R(x^i, x^j)$  is the correlation function between any two of the sample data points  $x^i$  and  $x^j$ . The correlation matrix considered in this paper is the common Gaussian correlation function,

$$\prod_{k=1}^n \exp(-\theta_k |d_k|)^2$$

where  $n$  is the number of design variables,  $\theta_k$  is the unknown correlation parameters used to fit the model and  $d_k$  is the distance between the  $k$ th component of sample points  $x^i$  and  $x^j$ .

The optimization algorithm in this approach is as follows:

- Initially some random designs are initialized. The procedure to identify these designs is to randomly choose the design points available with 50% on each sides of the initial population.
- The analysis code is run to construct the Kriging model for the two objective functions.
- The MOGA is performed on the Kriging model.
- If convergence is not achieved, additional random designs are chosen and the optimization process is repeated till convergence.

Further details of Kriging model are available in paper by Timothy, Timothy, John and Farrokh (1998).

## 4.2 NSGA II

An important aspect of this paper is the use of a multi-objective genetic algorithm NSGA-II developed by Deb, Agrawal, Pratap and Meyarivan (2002). This algorithm can give the full Pareto front for multi-objective problems. The merits and demerits of the classical gradient based approach and evolutionary approach for a given optimization problem are extensively discussed in literature by Lu and Zhenghong (2002) and Arora and Marler (2004). In a nutshell, the difficulties encountered by the classical optimization algorithm for general optimization problem occur in situations with (1) non-smooth variables, (2) nonlinear and discontinuous constraints, (3) noisy functions and (4) multiple minima. However, there are disadvantages in evolutionary optimization such as (1) no clearly defined convergence criteria, (2) parameter tuning mostly by trial and error, (3) computationally expensive population-based approach and (4) slow convergence to optimum. The main difference between classical optimization and evolutionary algorithm (EA) is that EA uses a population of solutions in each of the iterations, instead of a single solution. Since a population of solutions is processed in each of the iterations, the outcome of an EA is also a population of solutions.

When the optimization problem involves more than one objective function, the task of finding one or more optimum solutions is termed as multi-objective optimization as defined by Deb (2001). If the objective functions are conflicting in nature, each objective corresponds to a different optimal solution. Thus, there exist a set of optimal solutions where a gain in one objective calls for a sacrifice in some other objective. For a designer, knowing a number of optimal solutions becomes important and it also gives considerable insight into the design thereby providing several feasible and useful design solutions. Therefore, as far as the designer is concerned, the ideal multi-objective optimization procedure is to find the multiple trade-off optimal solutions with a wide range of values for the objectives and choose one of the obtained solutions using higher-level information. Often this higher-level information would be non-technical, qualitative and experience driven. Most of the multi-objective optimization algorithms use the concept of domination. This concept of domination is described in detail by Deb (2001).

The optimization model workflow is created in such a way that for a given starting value of design variables, it calculates the aerodynamic characteristics namely the lift, drag and moment coefficient. Using these coefficients, it maximizes the endurance of the UAV. Simultaneously, it generates the wing weight and checks for the violation of strength and stiffness constraints.

## 5 Results and Discussion

The low speed UAV under consideration has to loiter over the target area for many hours at a medium altitude. The all up weight of the UAV under consideration is 1800 Kg. It is a multi-mission UAV which has the capability to carry a variety of payloads in combinations depending on the mission. From the preliminary weight estimation, the empty weight fraction is 0.53 and the useful weight (payload weight and fuel weight) fraction is 0.47. The configuration of the UAV is twin engine wing mounted propeller driven tractor type. The UAV is powered by two piston propeller engine. The engine characteristics like the power at different altitudes, fuel consumption are captured in the propulsion module of the RDS. The fuel consumption of the engine selected is typical of any piston engines of this class which is of the order of 0.5 lbs/bhp/hr. The power data and its variation with altitude are inputted as given by the engine manufacturer. Similarly, the geometric data of propeller and its performance charts are inputted as supplied by the propeller manufacturer. The thrust generated by the propulsion module of RDS is corrected for the installation losses based on the experience of flying UAVs. The UAV belongs to the medium altitude long endurance category and hence flies at reasonably medium altitudes between 20,000 ft to 25,000 ft. It is a very low speed UAV whose cruise mach number is around 0.13. In this research, it is assumed that the UAV loiters at the same speed at same altitude for long hours. Hence the  $C_l$  is not changed considerably during loiter time.

For this study, in both single and dual objective problem, the following parameters are set for simulations in the genetic algorithm: Population size = 50, Number of generations = 100, Crossover probability = 0.9, Crossover distribution index = 20, Mutation probability = 0.1, Mutation distribution index = 100. For the kriging model construction, the number of random designs chosen is 20 and the number of additional random designs is 10. The optimization problem is performed on a PC with Windows XP platform and an Intel Pentium IV Processor with 2GB RAM and a processor speed of 1.86 GHz.

### 5.1 2D Airfoil Optimization

The baseline airfoil for aerodynamic optimization is the NASA/LANGLEY LS (1)-0417 (GA (W)-1). The airfoil is discretized into 100 panels in the XFLR5 code. The comparison of baseline and optimized airfoil geometric characteristics are given in Table 3.

As far as the 2D airfoil design optimization problem is concerned, Fig 4 shows the comparison of the airfoil geometry for the baseline and optimized design. It can be seen from Fig 4 and Table 3 that the thickness of the airfoil is increased from 17%

Table 3: Comparison of geometric characteristics of baseline and optimized airfoil

Characteristics	Baseline airfoil	Optimized airfoil
Maximum thickness to chord ratio	17%	18.9%
Maximum thickness position	30.2%c	26.7%c
Maximum camber	2.33%c	2.51%c
Maximum camber position	20.10%c	21.3%c
Trailing edge gap	0.73%c	0.67%c

to 18.9%. The optimized airfoil has slightly better characteristics in terms of area enclosed by the airfoil, which is a measure of the total internal volume available for fuel storage between the spars. The optimized airfoil maintains almost same camber of the seed airfoil as 2.51%c while the leading edge curvature is reduced from 28.94% to 18.42%. The trailing edge angle is increased slightly from 3.19° to 4.62° in order to reduce the constraint imposed on structural stiffness of the airfoil. Figs. 5-7 present the lift, drag and endurance parameter. It can be clearly seen from Fig 5-7 and Table 4 that the aerodynamic characteristics of the optimized airfoil are much better when compared to the baseline airfoil. The  $C_{lmax}$  has increased by 13.5% and the maximum endurance parameter has increased by 43.5%.

Table 4: Comparison of performance characteristics of baseline and optimized airfoil

PARAMETER	Baseline airfoil	Optimized airfoil
$C_{lmax}$	1.85	2.1
$C_{l0}$	0.55	0.55
Alpha – max in deg	19	17
Alpha 0 in deg	-4	-4
$C_l$ -alpha (Linear range) per deg	0.1125	0.1175
$C_{d0}$ at alpha = 0	0.005	0.005
$C_{m0}$	-0.12	-0.09
Max Endurance Parameter	108	155

## 5.2 3D Wing Planform Optimization

At the end of the 2D airfoil optimization, the maximum thickness to chord ratio and the camber are frozen at the values obtained from the optimization process. Once the airfoil cross section is frozen, the wing planform is optimized as the next step. During this step, the wing planform parameters aspect ratio, wing loading, taper ra-

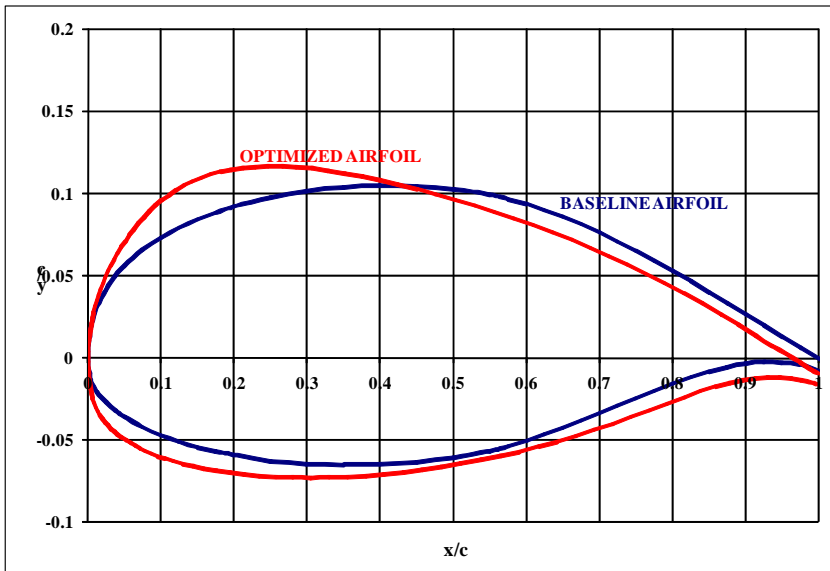


Figure 4: Geometry of baseline and optimized airfoil

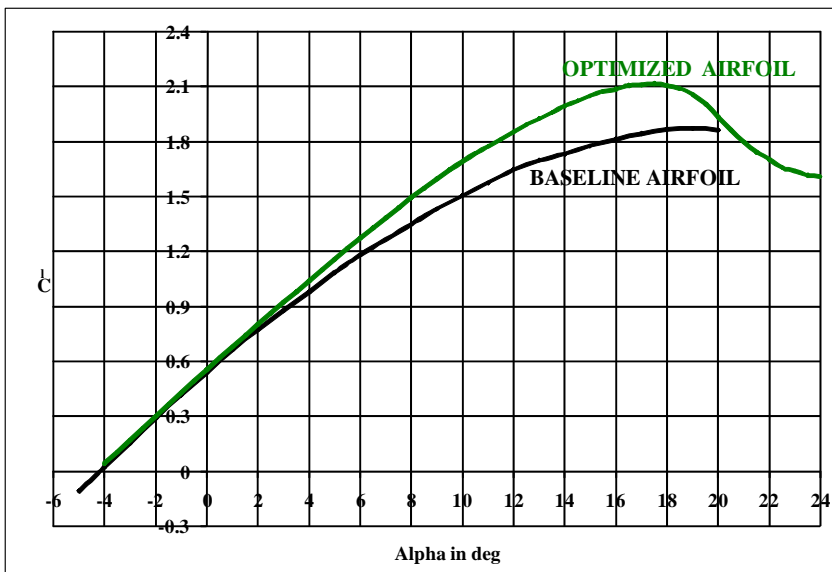


Figure 5: 2D Lift characteristics for baseline and optimized airfoil

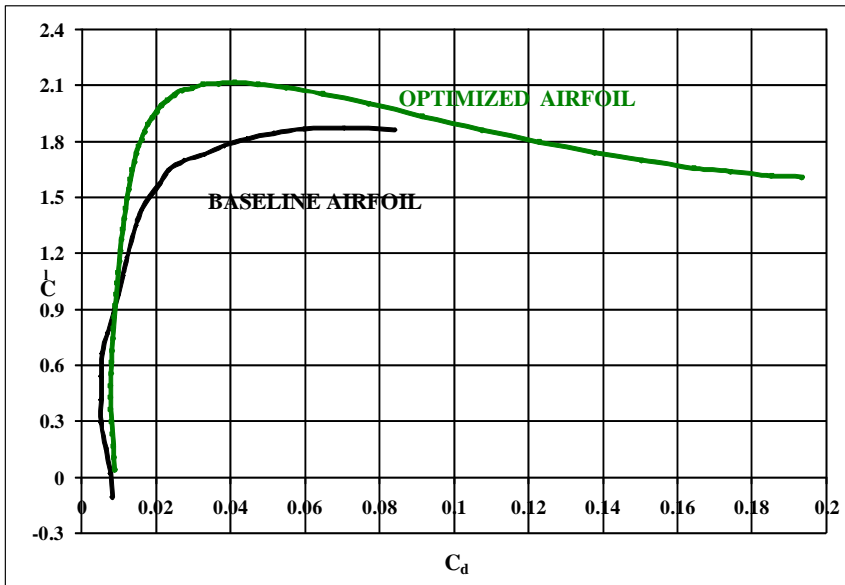


Figure 6: 2D Drag characteristics for baseline and optimized airfoil

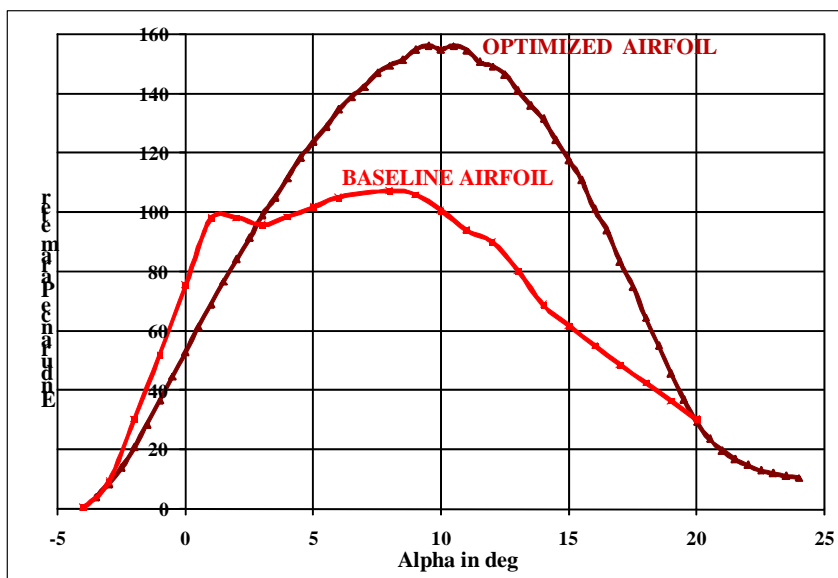


Figure 7: Endurance parameter for baseline and optimized airfoil

tio, wing twist angle are optimized subject to performance constraints. Apart from the wing planform parameters, the design variables from the structures discipline such as the skin thickness at root and tip are also considered.

The lift and drag characteristics of the optimum airfoil obtained using the XFLR5 code is presented in Fig 8 and 9, respectively.

The structural analysis results obtained using finite element analysis are presented in Figs 10-11. The strength and stiffness constraints are active during the 3D wing planform optimization. The maximum value of the stress coming on the entire wing structure is estimated by the finite element analysis and is compared with the allowable stress value of the material. The maximum deflection coming on the tip of the wing is estimated during the finite element analysis and is compared with the maximum allowable deflection value as per the AVP 970 standard.

For the 3D wing design optimization problem, a graph between the two objectives namely given by the wing weight and endurance parameter is plotted to obtain the Pareto front shown in Fig 12.

It is a typical Min-Max Pareto front. Five design solutions are possible with optimum solutions lying in the Pareto front. These Pareto points are designated with PP1 to PP5. The design variables corresponding to the two extreme Pareto points PP1 and PP5 are described in Table 5, along with the objective function value corresponding to that point.

Table 5: Design Variables corresponding to Pareto points PP1 and PP5

<b>Design Variables</b>	<b>Pareto Point PP1</b>	<b>Pareto Point PP5</b>
Wing Aspect Ratio	0.82	0.98
Wing Loading	0.99	0.91
Wing Taper Ratio	0.3125	0.45
Wing twist angle	0.4	0.93
Upper skin thickness at root	0.73	0.92
Upper skin thickness at tip	0.37	0.44
Lower skin thickness at root	0.73	0.92
Lower skin thickness at tip	0.37	0.44
Wing Weight	0.067	0.105
Endurance parameter	0.4	0.92

Fig 13 to Fig 20 presents the optimal values of the seven design variables corresponding to each of the five Pareto points given in Fig 12. There is a variation of about 15 percent in the aspect ratio as shown in Figure 13 between the different designs. The wing loading in Figure 14 shows a variation of about 9 percent with

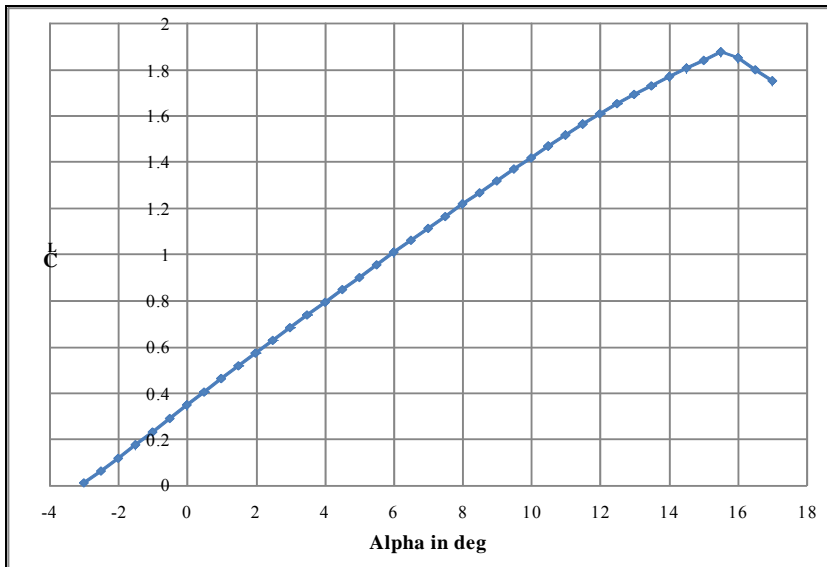


Figure 8: 3D Lift characteristics for optimum airfoil

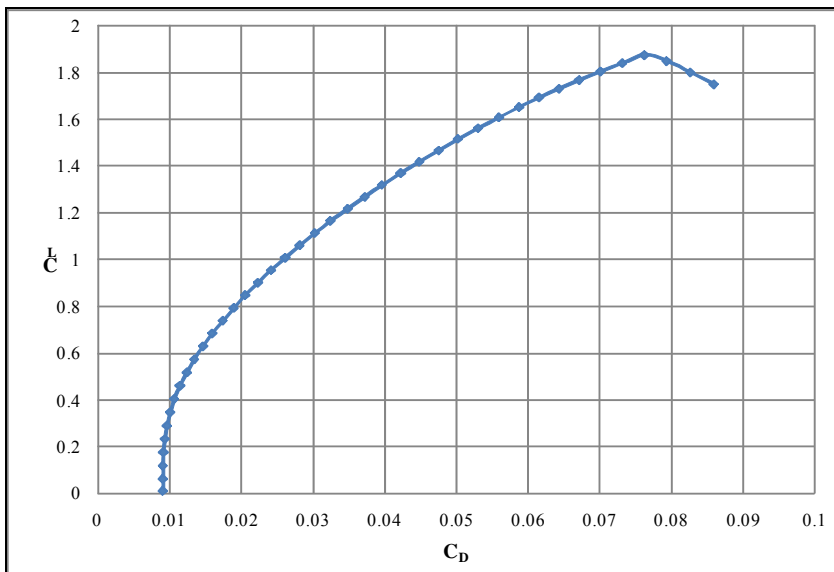


Figure 9: 3D Drag characteristics for optimum airfoil



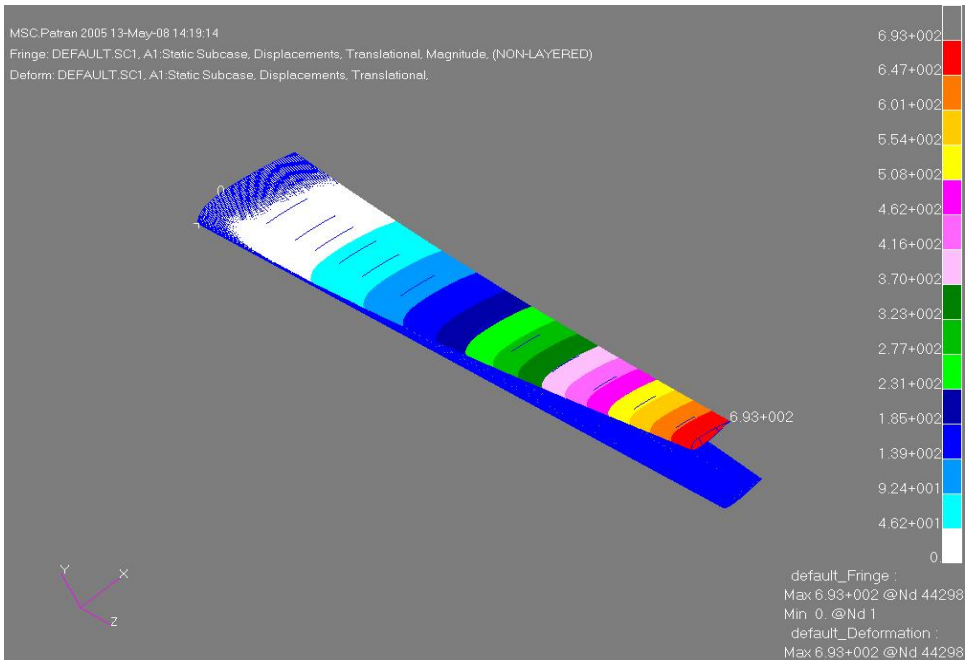


Figure 10: Displacement contour of the optimized 3D wing

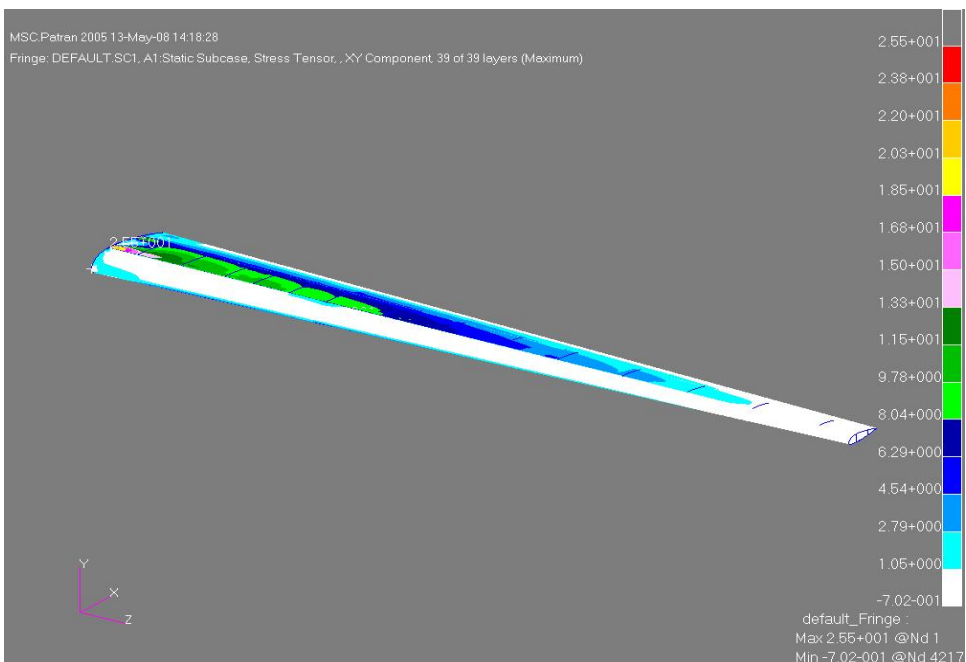


Figure 11: Stress contour of the optimized 3D wing

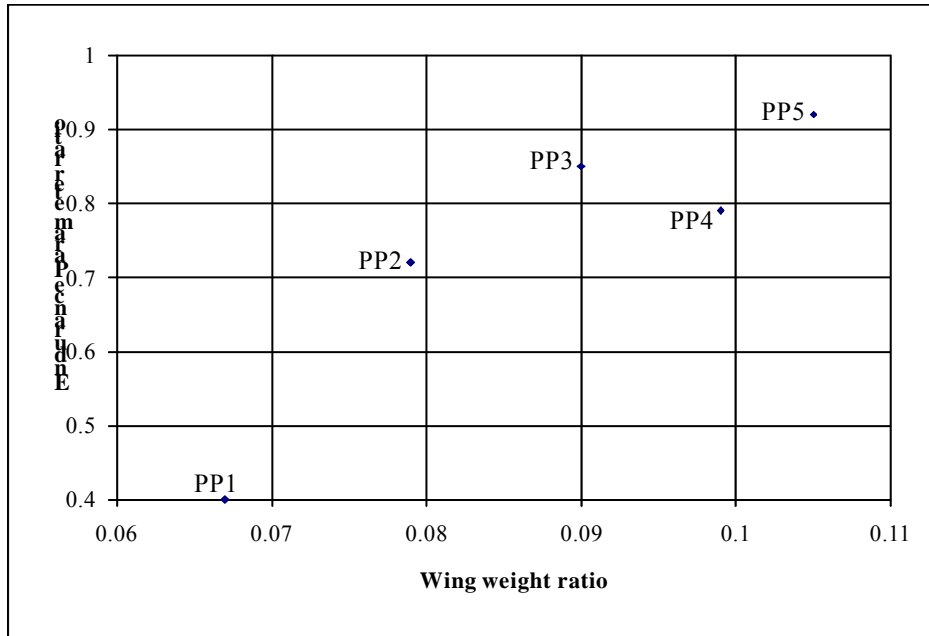


Figure 12: Pareto front obtained using the multi objective genetic algorithm

two values near the maximum bound. The taper ratio in Figure 15 shows a large variation of over 64 percent, however, none of the designs show the taper ratio at the upper bound. The wing twist shows a variation of about 57 percent between the maximum and minimum values and none of the designs reach the upper limit which is also a substantial variation. There is also a considerable variation in wing upper and lower skin thickness at root between the Pareto designs of about 26 percent with one design being very close to the upper limit. Finally, wing upper and lower skin thickness at tip shows a marginal variation of about 15 percent with no design reaching the upper limit.

There is a large variation in the design variables between the five Pareto points. The different planform shapes corresponding to the five Pareto points are shown in Fig 21. These planform shapes offer choice to the designer interested in experimenting with different plan form shapes and sizing and also for structural design. The identification of the Pareto front gives considerable insight into the design problem. The Pareto points for the preliminary design can now be evaluated for use in detailed structural wing design studies.

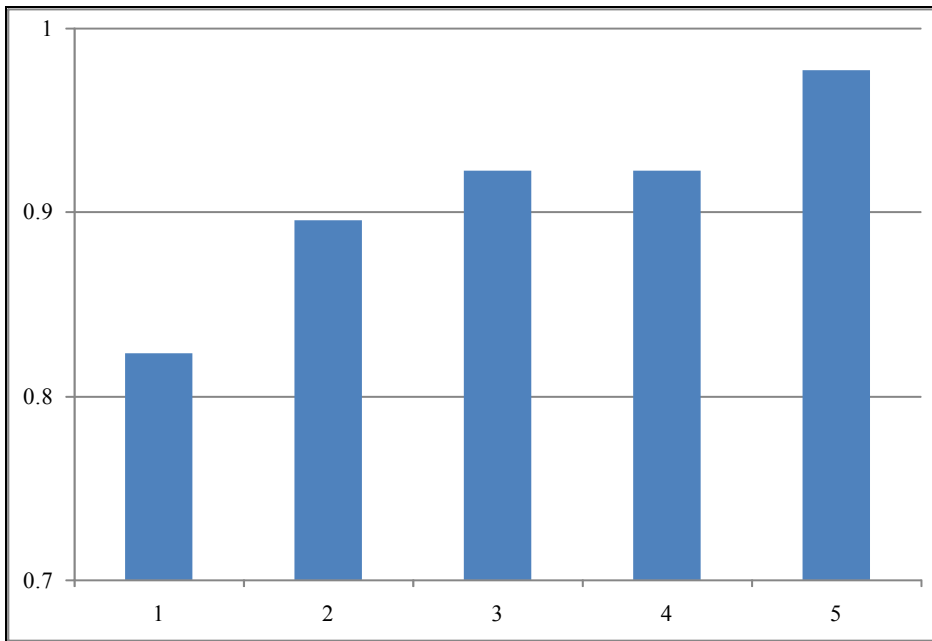


Figure 13: Aspect Ratio for different Pareto points

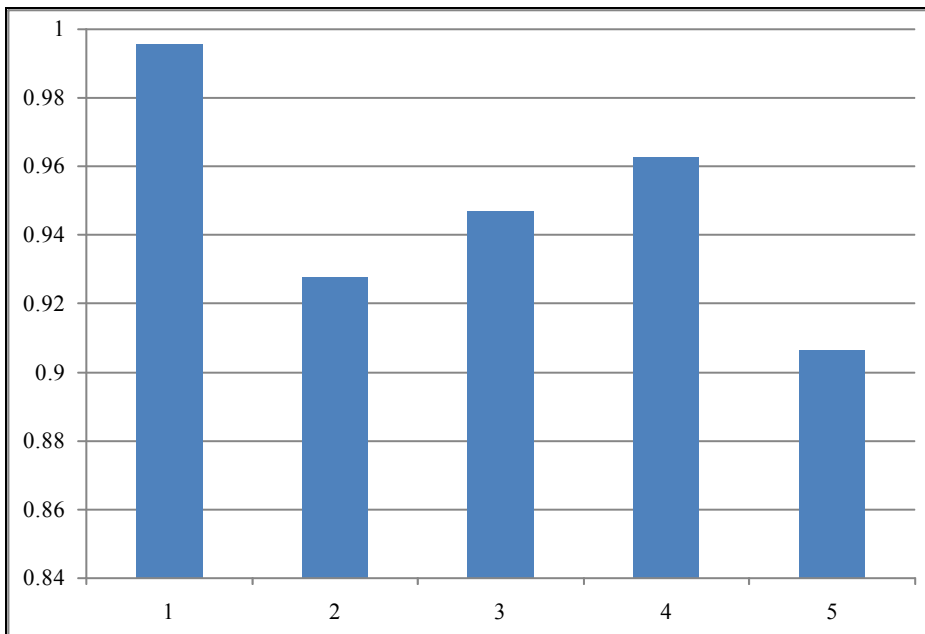


Figure 14: Wing Loading for different Pareto points

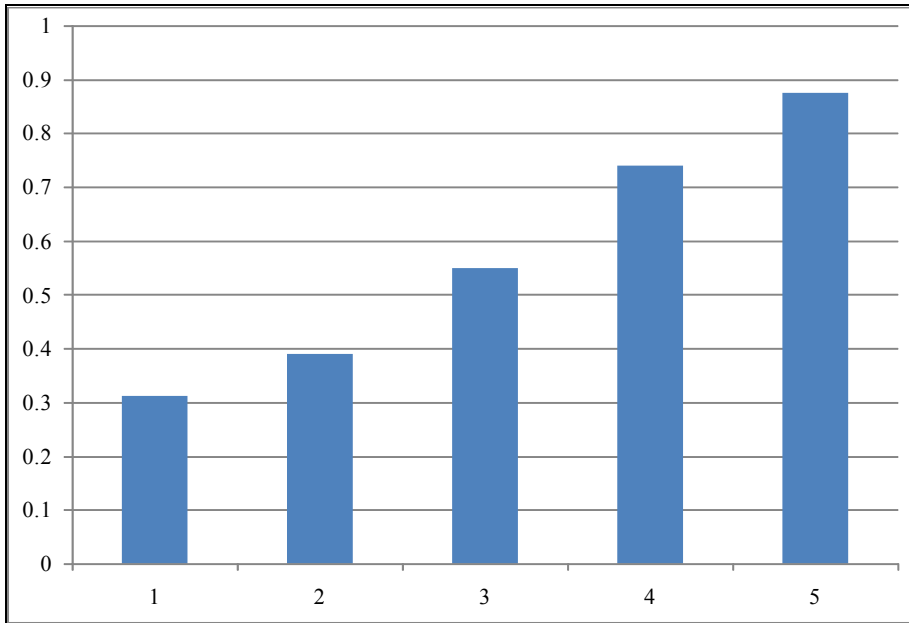


Figure 15: Taper Ratio for different Pareto points

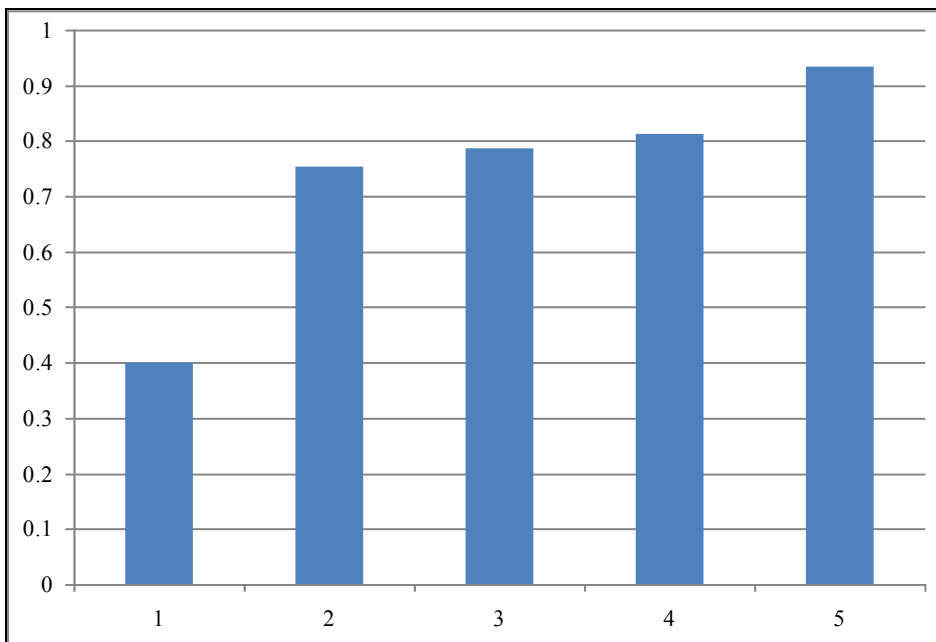


Figure 16: Wing Twist for different Pareto points

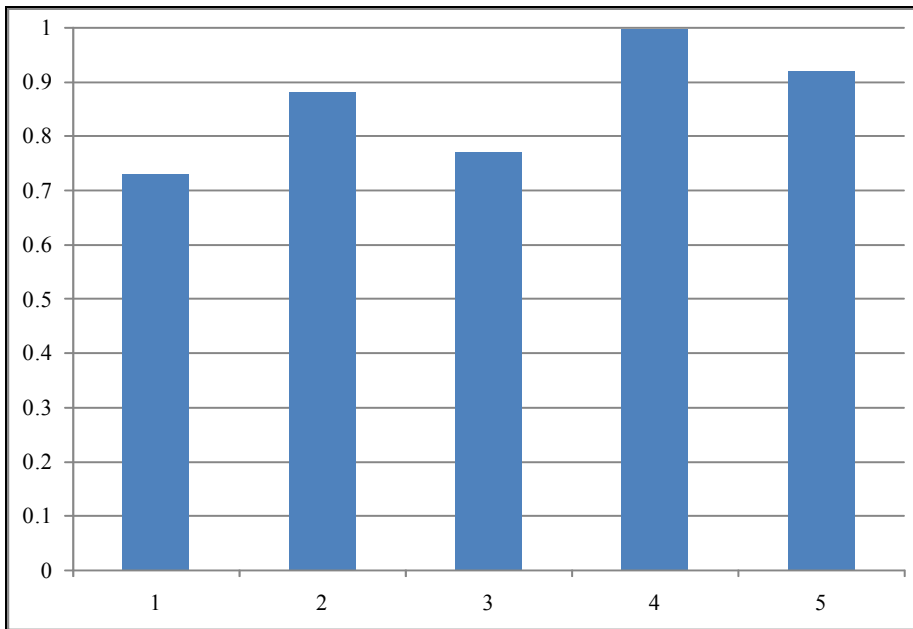


Figure 17: Wing upper skin thickness at root for different Pareto points

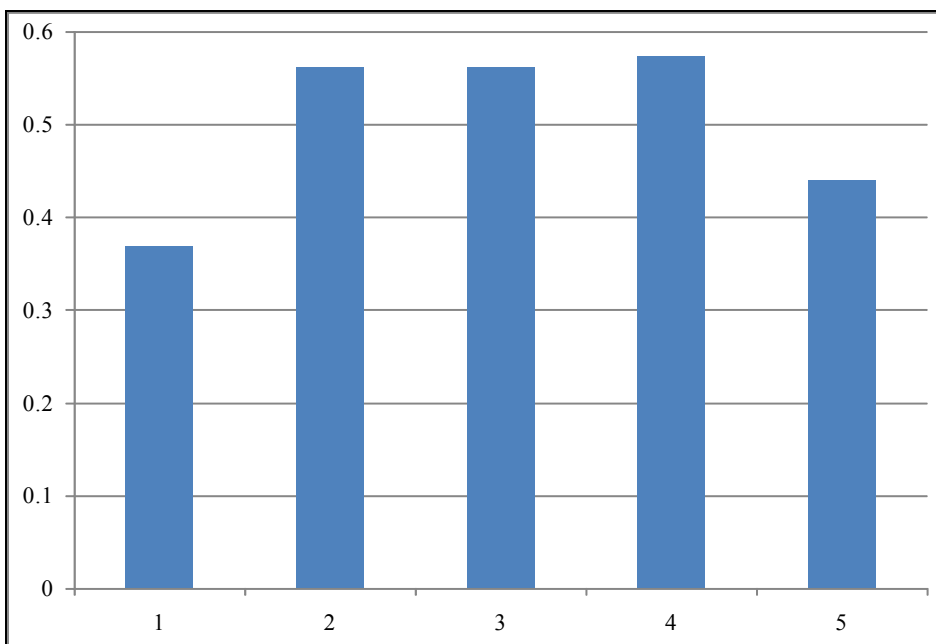


Figure 18: Wing upper skin thickness at tip for different Pareto points

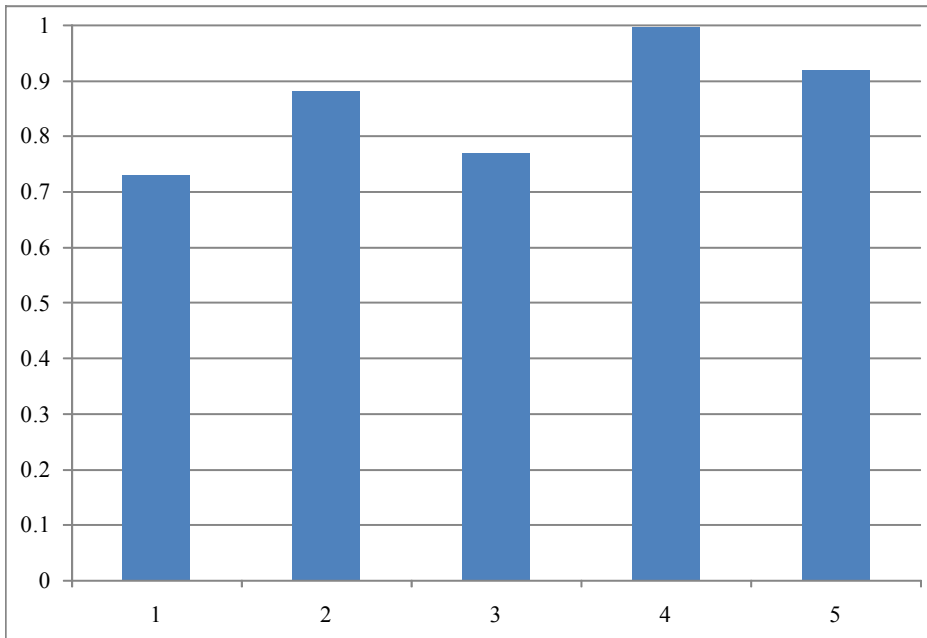


Figure 19: Wing lower skin thickness at root for different Pareto points

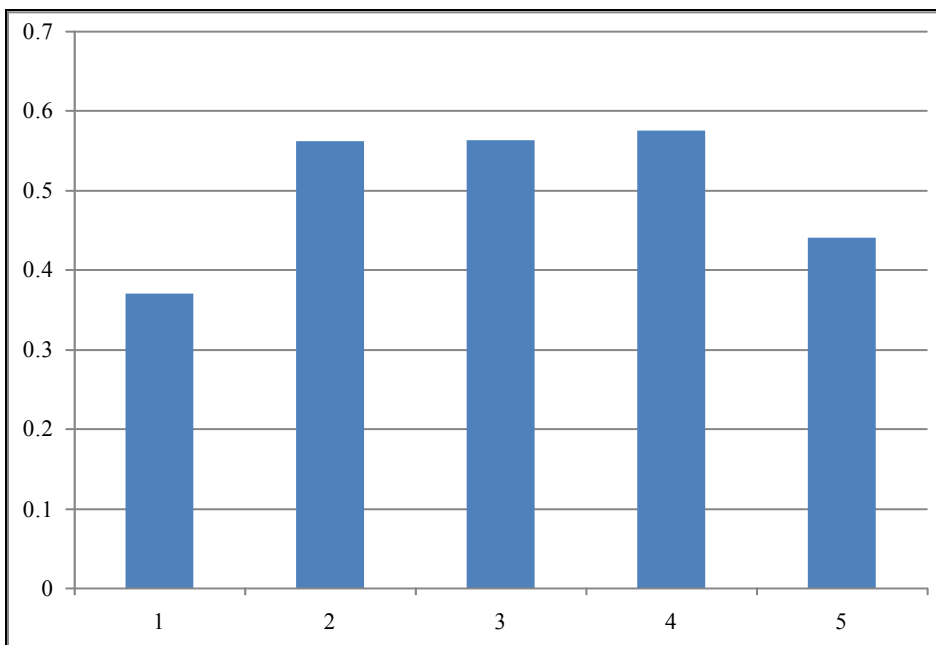


Figure 20: Wing lower skin thickness at tip for different Pareto points

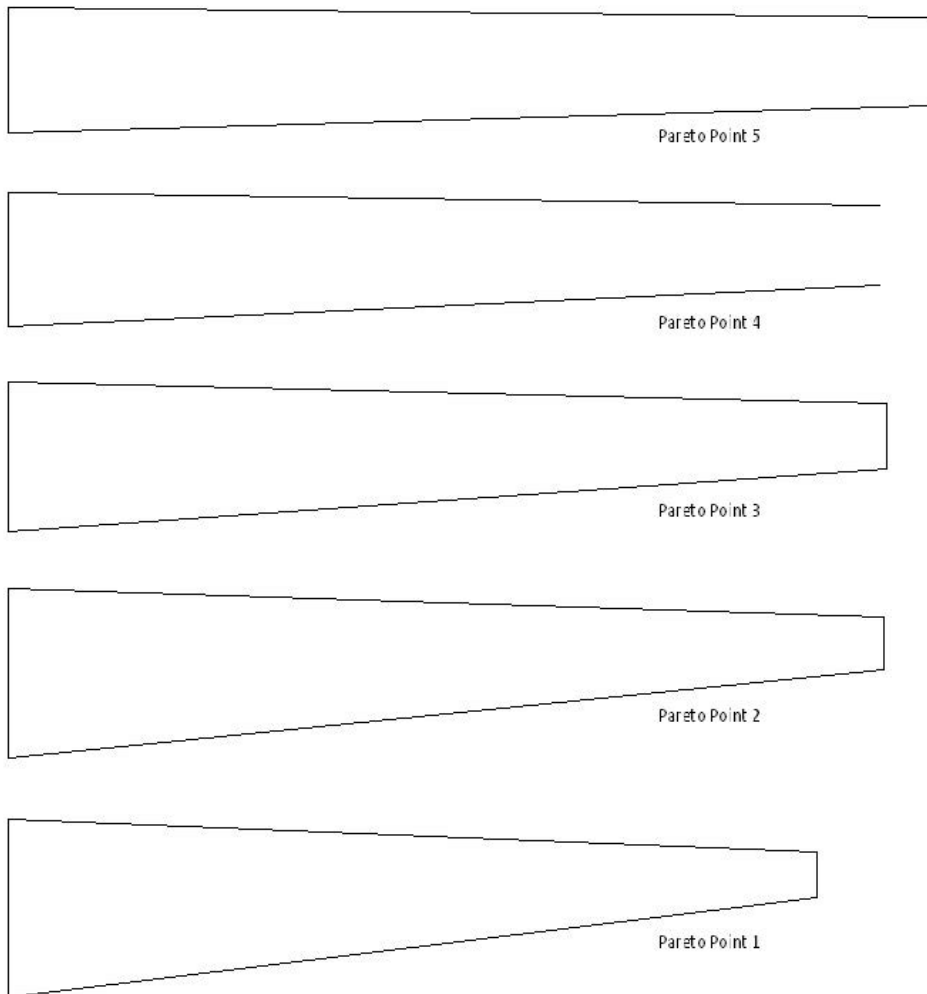


Figure 21: Planform shapes for different Pareto points

## 6 Conclusions

An evolutionary optimization algorithm capable of finding the full Pareto front of multi-objective optimization problems is applied for preliminary UAV wing design. The preliminary design problem is formulated as a mathematical optimization problem. A single objective problem of maximizing the endurance parameter and a dual objective problem of maximizing endurance parameter and minimizing wing weight is considered. The formulation and workflow is done in two steps,

initially a 2D airfoil optimization where the airfoil geometry is optimized to give a maximum endurance parameter with constraints on geometrical parameters. In the second step, the 3D wing planform is optimized with objective functions from aerodynamics and structures. In the second step, the Kriging approximation model, replaces both the aerodynamic and structural analysis code. The robust evolutionary algorithm NSGA-II used to capture the Pareto front is capable of identifying the trade-off between the conflicting objectives thereby providing alternative useful designs for the designer. It is found that the five Pareto designs obtained offer various possibilities to the designer in terms of higher-level requirement and may offer novel and non-traditional solutions to the design problem. The Kriging model employed reduces the computation time without losing the Pareto points. The optimization results confirm the feasibility of the Kriging based MOGA for UAV wing design optimization and provide useful starting points for detailed structural design of the UAV wing.

**Acknowledgement:** The authors gratefully acknowledge the support given by all colleagues who have helped directly and indirectly in carrying out this work and Director, ADE (DRDO) for permitting the paper to be published.

## References

- Arora J. S., Marler R. T.** (2004): Survey of multi-objective optimization methods for engineering, *Structural and Multidisciplinary Optimization*, 26, pp. 369-395.
- Bartholomew, P.** (1998): The Role of Aerospace design and progress towards an MDO capability, AIAA Paper No. 98-4705.
- Carrier, G.** (2004): Multidisciplinary Design Optimization of a supersonic transport aircraft wing planform, *ECCOMAS 2004*.  
Dassult Systems, "CATIA V5R17 Documentation".
- Deb, K.** (2001): *Multi Objective Optimization using Evolutionary Algorithms*, Chichester, UK:Wiley.
- Deb K., Srinivas N.** (1994): Multi Objective Optimization using Non Dominated Sorting Genetic Algorithm", *Journal of Evolutionary Computation*, 2 (3) pp. 221-248.
- Deb K., Agrawal S., Pratap A., Meyarivan T. A.** (2002): A Fast and Elitist Multi Objective Genetic Algorithm: NSGA-II, *IEEE Transactions on Evolutionary Computation*, 6 (2) pp. 182-197. Guidelines for XF5R5 V2.00 Rev 5.
- Dovi A.R., Wrenn G.A.** (1990): Aircraft design for mission performance using nonlinear multi-objective optimization methods, *Journal of Aircraft*, 27(12) pp.



1043-1049.

**Drela M.** (2001) XFOIL 6.94 User guide, MIT Department of Aeronautics and Astronautics.

**Goldberg D.E.** (1989): *Genetic Algorithms in Search, Optimization and Machine Learning*, Addison Wesley Pub Co., Reading, MA.

**Grossman, B., Haftka, R.T., Kao, P.J., Polen, D.M., Rais-Rohani, M.** (1990): Integrated aerodynamic-structural design of a transport wing, *Journal of Aircraft*, 27 (12) pp. 1050-1056.

**Gonzalez, L.F., Lee, D.S., Srinivas, K., Wong, K.C.** (2006): Single and multi-objective UAV aerofoil optimization via hierarchical asynchronous parallel evolutionary algorithm, *The Aeronautical Journal*, 110 (1112) pp. 659-672.

**Gonzalez, L.F., Periaux, J., Srinivas, K., Whitney, E.J.** (2006): A Generic Framework for Design Optimization of Multidisciplinary UAV Intelligent Systems using Evolutionary Computing, 44<sup>th</sup> AIAA Aerospace Sciences Meeting and Exhibit, Reno, NV, USA.

**Jeong S., Murayama M., Yamamoto K.** (2005): Efficient optimization design method using Kriging model, *Journal of Aircraft*, 12 (2) pp. 413-420.

**Kim Y., Jeon Y.H., Lee D.H.** (2006): Multi-objective and multidisciplinary design optimization of supersonic fighter wing, *Journal of Aircraft*, 43 (3) pp. 817-824.

**Kipouros, T, Jaeggi, D. M., Dawes, W. N., Parks, G. T., Savill, A. M., Clarkson, P. J.** (2008): Insight into High-quality Aerodynamic Design Spaces through Multi-objective Optimization, *CMES: Computer Modeling in Engineering & Sciences*, 37 (1), pp. 1-44.

**Kroo. I.** (1997): Multidisciplinary Optimization Applications in Preliminary Design, 38<sup>th</sup> AIAA/ASME/ASCE/AHS/ASC Structures, Structural Dynamics and Materials Conference, Kissimmee, Florida.

**Kumano T., Jeong S., Obayashi S.** (2006): Multidisciplinary Design Optimization of Wing Shape for a small Jet Aircraft Using Kriging Model, AIAA 2006-932.

**Lee, D.S., Gonzalez, L.F., Srinivas, K.** (2008): Robust evolutionary algorithms for UAV/UCAV aerodynamic and RCS design optimisation, *Computers and Fluids*, 37 (5) pp. 547-564.

**Lu X., Zhenghong G.** (2002): The investigation of multi-disciplinary and multi-objective optimization method for the aircraft configuration design, ICAS Paper No 2002-811.1.

**Martins J.R.R.A., Alonso J.J.** (2002): Complete configuration aero-structural optimization using coupled sensitivity analysis method", AIAA 2002-5402.

MSC Software Inc., MSC Nastran User Guide and Reference manuals, URL: <http://www.mscsoftware.com/>.

MSC Software Inc., MSC Patran User Guide and Reference manuals, URL: <http://www.mscsoftware.com/>.

**Morino L., Bernardini G., Mastroddi F.** (2006): Multi-disciplinary optimization for the conceptual design of innovative aircraft configurations, *CMES: Computer Modeling in Engineering & Sciences*, 13 (1), pp. 1-18.

**Rajagopal S., Ganguli R., Pillai A.C.R., Lurdharaj A.** (2007): Conceptual Design of Medium Altitude Long Endurance UAV using Multi Objective Genetic Algorithm, *AIAA 2007-1885*.

**Raymer D. P.** (1992): *Aircraft Design: a Conceptual Approach*, AIAA Education series, AIAA, Washington DC.

**Sobieski I., Haftka R.T.** (1996): Multidisciplinary Aerospace Design Optimization: Survey of Recent Development, *AIAA Paper No. 96-0711*.

**Sobester A., Keane A.J.** (2006): Multidisciplinary Design Optimization of UAV Airframes, *AIAA 2006-1612*.

**Srinath. D. N., Mittal. S.** (2009): Optimal airfoil shapes for low Reynolds number flows, *International Journal for Numerical Methods in Fluids*, 61 (4), pp. 355-381

**Timothy W. S, Timothy M. M., John J. K., Farrokh M.** (1998): Comparison of response surface and kriging models for MDO, *AIAA Paper No. 98-4755*.

**Wakayama, S., Kroo, I.** (1995): Subsonic wing planform design using multidisciplinary optimization, *AIAA Journal*, 32 (4) pp. 746-753.